

Article

Effects of Prescribed Burning on Surface Dead Fuel and Potential Fire Behavior in *Pinus yunnanensis* in Central Yunnan Province, China

Jin Wang ¹, Ruicheng Hong ¹, Cheng Ma ¹, Xilong Zhu ¹, Shiying Xu ¹, Yanping Tang ², Xiaona Li ³, Xiangxiang Yan ⁴, Leiguang Wang ^{5,*} and Qiuhua Wang ^{1,*}

¹ College of Civil Engineering, Southwest Forestry University, Yunnan Key Laboratory of Forest Disaster Warning and Control, Kunming 650224, China; wangjin20210630@163.com (J.W.); hrc13700635230@163.com (R.H.); 18468220368@163.com (C.M.); zjgxl520233@gmail.com (X.Z.); xushiyng6666@163.com (S.X.)

² College of Life Sciences, Southwest Forestry University, Kunming 650224, China; typ1872739499@163.com

³ College of Geography and Eco-Tourism, Southwest Forestry University, Kunming 650224, China; xiaonali_20060429@163.com

⁴ Kunming Forest Fire Control and Forestry and Grass Information Center, Kunming 650500, China; yxx2385166186@163.com

⁵ Institute of Big Data and Artificial Intelligence, Southwest Forestry University, Kunming 650024, China

* Correspondence: leiguangwang@swfu.edu.cn (L.W.); qhwang2010@swfu.edu.cn (Q.W.); Tel.: +86-137-6913-3908 (Q.W.)



Citation: Wang, J.; Hong, R.; Ma, C.; Zhu, X.; Xu, S.; Tang, Y.; Li, X.; Yan, X.; Wang, L.; Wang, Q. Effects of Prescribed Burning on Surface Dead Fuel and Potential Fire Behavior in *Pinus yunnanensis* in Central Yunnan Province, China. *Forests* **2023**, *14*, 1915. <https://doi.org/10.3390/f14091915>

Academic Editor: Rosemary Sherriff

Received: 15 August 2023

Revised: 7 September 2023

Accepted: 18 September 2023

Published: 20 September 2023



Copyright: © 2023 by the authors. Licensee MDPI, Basel, Switzerland. This article is an open access article distributed under the terms and conditions of the Creative Commons Attribution (CC BY) license (<https://creativecommons.org/licenses/by/4.0/>).

Abstract: Prescribed burning is a widely used fuel management employed technique to mitigate the risk of forest fires. The *Pinus yunnanensis* Franch. forest, which is frequently prone to forest fires in southwestern China, serves as a prime example for investigating the effects of prescribed burning on the flammability of surface dead fuel. This research aims to establish a scientific foundation for managing dead fuel in forests, as well as fire prevention and control strategies. Field data was collected from *P. yunnanensis* forests located in central Yunnan Province in 2021 and 2022. The study implemented a randomized complete block design with two blocks and three treatments: an unburned control (UB), one year after the prescribed burning (PB1a), and three years after the prescribed burning (PB3a). These treatments were evaluated based on three indices: surface dead-bed structure, physicochemical properties, and potential fire behavior parameters. To analyze the stand characteristics of the sample plots, a paired *t*-test was conducted. The results indicated no significant differences in the stand characteristics of *P. yunnanensis* following prescribed burning ($p > 0.05$). Prescribed burning led to a significant decrease in the average surface dead fuel load from 10.24 t/ha to 3.70 t/ha, representing a reduction of 63.87%. Additionally, the average fire-line intensity decreased from 454 kw/m to 190 kw/m, indicating a decrease of 58.15%. Despite prescribed burning, there were no significant changes observed in the physical and chemical properties of dead fuels ($p > 0.05$). However, the bed structure of dead fuels and fire behavior parameters exhibited a significant reduction compared with the control sample site. The findings of this study provide essential theoretical support for the scientific implementation of prescribed burning programs and the accurate evaluation of ecological and environmental effects post burning.

Keywords: prescribed burning; *Pinus yunnanensis*; fuel characteristics; forest fire management; surface fire; fire behavior

1. Introduction

The escalating impact of global warming is exacerbating hot and arid conditions, thereby increasing the potential hazards of forest fires in various regions and posing risks to forest functionality [1]. However, it is important to note that forest fires also constitute a significant disturbance mechanism in forest ecosystems and contribute to forest

growth and development [2]. In this context, dead fuels constitute the source of forest fires and are the bedrock of fire behavior, impacting fire suppression difficulty, fire-line intensity, fire severity, and post-fire losses [3]. Consequently, wildfire managers require detailed information on fuel-burning characteristics to effectively mitigate wildfire risks. Quantitative investigation into the combustibility of deceased fuels is fundamental to modern wildland fire management. This research holds significant practical importance in predicting the occurrence and behavior of wildland fires, as well as in the direction of managing fire suppression and using fire in camp forests. Additionally, alongside essential conditions such as oxygen and an ignition source, combustion can be influenced by physicochemical properties, such as ash content, moisture content, and so forth [4].

Pinus L. is a largely northern hemisphere genus distributed across many forest types in Europe, Asia, North Africa, North America, and Central America [5], with most of its distribution in fire-prone habitats [6]. China is one of the distribution centers for *Pinus*. There are twenty-two species of pine, including *Pinus yunnanensis* Franch., which are distributed in the center of the central plateau of Yunnan and the northwest regions of Guangxi, Guizhou, Sichuan, and Tibet, as shown in Figure 1 [7]. The region exhibits an elevation range from 600 m to 3100 m and is an irregularly shaped polygon. It holds substantial potential for carbon sequestration, with the tree and soil layers serving as the primary carbon storage of the forest ecosystem [8]. In central Yunnan, influenced by the monsoon climate monsoon climate, *P. yunnanensis* thrives as the predominant indigenous tree species in fire-prone habitats, showcasing a “fire-dependent” life-history response, that has facilitated its status as the most common endemic tree species in the region’s fire-prone habitats [9]. Thus, studying the effect of prescribed burning on the combustibility of dead fuels in *P. yunnanensis* forests can lead to a better understanding of its fire behavior and adaptation to periodic fires and the development of reasonable regulations. This research is crucial to predicting *P. yunnanensis* forest fires, understanding fire behavior, and ensuring the safe suppression of fires.

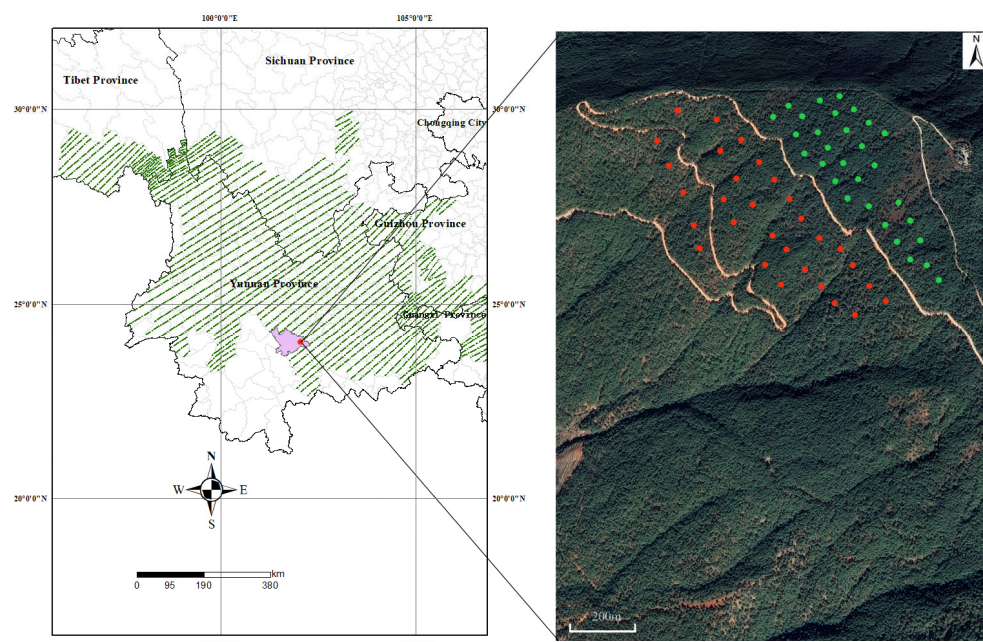


Figure 1. The distribution area of *Pinus yunnanensis* in China. On the right side of the figure, red dots indicate the prescribed burning (PB) sample sites and green dots represent the unburned (UB) sample sites.

Prescribed burning is a widely employed technique used in fire-prone forests to modify the structure of the forest stand, reducing the likelihood of severe wildfires and bolstering ecosystem resilience to natural disturbances [10]. By reintroducing fire to the forest ecosys-

tem, which removes dead fuels that have accumulated in the understory, reduces forest flammability and fosters favorable soil and stand conditions that promote stand regeneration [11]. Numerous studies have shown that prescribed burns exert minimal influence on the mature canopy, while concurrently fostering seedling recruitment and contributing to the restoration of biodiversity [12–14]. Prescribed burning does not significantly impact seed production, seedling germination, and seedling mortality in the long term [15]. In addition, it is more effective in reducing the magnitude of simulated wildfires [16]. Furthermore, it plays a crucial role in mitigating the risk of high-intensity fires and curbing large-scale biomass burning, thereby helping to minimize CO₂ emissions [17,18]. The accumulation of leaf litter in *P. yunnanensis* forests starts to level off around the sixth year and gradually reaches a state of equilibrium [19], leading to the build-up of combustible dead fuel on the forest floor, escalating the risk of wildfire. The complete exclusion of fire in *P. yunnanensis* forests is scientifically unsound. Conversely, prescribed burning can be effective in reducing the potential for surface fires to spread into forest crown fires [20]. Nevertheless, the effects of prescribed burning on ecosystems and climate are complex and carry risks [21]. These risks encompass various aspects, including impacts on forest stands [22], air pollutants [23], soil properties [11,24–26], biodiversity [27–29], and surface dead fuels [30,31].

Currently, the research on the effects of prescribed burning mainly focuses on the boreal region [32,33], including the western of North America, Russia, Siberia, and the Daxing'anling region in China. However, there is still a lack of understanding regarding the impact of forest fire disturbance on dead fuel dynamics in subtropical coniferous forest areas, particularly in the high-altitude regions of the northern subtropical plateau with a monsoon climate. In contrast to the fire-prone habitats in the Mediterranean-type climate, characterized by distinct dry and wet seasons [34], *P. yunnanensis* forests are distributed in the subtropical region where the hot and humid seasons coincide. Nevertheless, the climate remains fire prone with distinct dry and wet seasons [35]. This study focuses on examining the bed structure, physicochemical properties, and potential fire behavior characteristics of dead fuels on the surface of *P. yunnanensis* after prescribed burns. The objective of this research is to offer valuable insights for sustainable forest management in subtropical low-latitude and high-altitude areas.

2. Materials and Methods

2.1. Description of the Study Area

Xinping County is situated in the southwest of central Yunnan Province, at an elevation between 23°38'15"–24°26'05" N and 101°16'30"–102°16'50" E, and covers a total area of 4223 sq. km. The region's topography is predominantly mountainous and accounts for 98.03% of the area, with high elevations in the northwest and low ones in the southeast. The local climate is affected by the region's altitude and falls under three different climate types: subtropical, high-temperature river valley area, mid-mountain warm temperature zone, and high-mountain cold temperature zone. The region experiences an average annual temperature of 18.1 °C, with maximum and minimum temperatures of 32.8 °C and 1.3 °C, respectively. The average yearly precipitation is 869 mm, and there are 2838.7 h of sunshine per year [36].

Xinping County, situated in central Yunnan, has the highest risk of wildfires. The primary coniferous tree species is *P. yunnanensis*. The understory shrubs are scarce, with common species such as *Vaccinium bracipedicellatum* Thunb, *Rhododendron spiciferum* Franch, *Quercus aliena* Blume, and *Schima khasiana* Dyer. The herbaceous plants are more plentiful and chiefly composed of grass species, including *Festuca ovina* L., *Agrostis matsumurae* Trin., *Schizachyrium brevifolium* Nees ex Buse., *Heteropogon contortus* (L.) P. Beauv. ex Roem. et Schult., *Cymbopogon distans* (Nees.) Wats., *Eulalia speciosa* (Debeaux) Kuntze., and *Ainsliaea plantaginifolia* Mattf., among others.

2.2. Field Sampling Description

In December 2021 and December 2022, respectively, systematic observations were conducted to assess changes in the stand structure of pure *P. yunnanensis* stands at specific locations ($24^{\circ}2'10''$ N~ $24^{\circ}0'30''$ N, $102^{\circ}0'30''$ E~ $102^{\circ}1'20''$ E) following prescribed burns. As shown in Figure 1, the study implemented a randomized complete block design with two blocks including prescribed burning sample plots (PB) and unburned control sample plots (UB), and three treatments: unburned control, one year after the prescribed burning (PB1a), and three years after the prescribed burning (PB3a). These treatments were evaluated based on three indices: surface dead-bed structure, physicochemical properties, and potential fire behavior parameters.

Each sample plot was $10\text{ m} \times 10\text{ m}$, and 30 pieces of each type of sample plot were set up, resulting in a total of 60 sample plots. Each sample plot was recorded in detail, including geographic location along with slope, slope direction, slope position, and other topographic elements. The number of trees, their height (obtained using a portable tree height meter, DZH-30), diameter at breast height (DBH), under-branch height, and the number and height of shrubs and herbs in each sample plot were recorded. Table 1 provides the essential characteristics of the sample plots. Five surface dead combustible samples were set up in each sample plot (Figure 2a), and collected for indoor experiments [37].

Table 1. Standing conditions and tree growth of *P. yunnanensis* in the study area by varied treatments.

Treatment	Altitude (m)	Slope ($^{\circ}$)	Overstory Cover (%)	Tree Density ² (No./ha)	DBH (cm)	Height (m)	Under-Branch Height (m)
							Mean (SE) ¹
UB	2010–2050	6–25	0.47	1481	17.1 (1.0)	11.0 (1.3)	5.7 (1.6)
PB1a			0.54	1170	16.5 (0.8)	10.3 (2.1)	7.3 (1.2)
PB3a	1800–2000	10–37	0.55	1198	17.1 (1.3)	11.3 (1.5)	7.6 (1.4)

¹ Mean and one standard error (SE). ² Tree density for trees greater than 7.5 cm diameter.

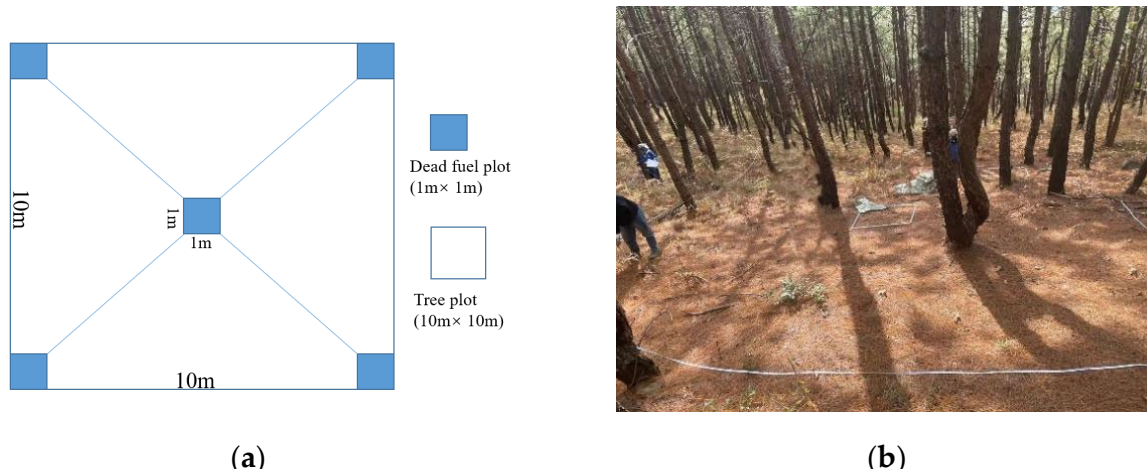


Figure 2. (a) Schematic diagram of the survey sample site, in which the number and height of trees in the tree plot were surveyed, and all combustibles in the dead fuel plot were collected; (b) an example of measurement plot.

2.3. Sample Analysis

The following experiments were conducted, and the results were obtained in the laboratory under standard temperature and pressure conditions.

2.3.1. Determination of FMC

To complete desiccation, we placed the collected samples in an electrically heated oven and baked them continuously at temperatures between 85 °C and 105 °C for 24 h. We determined the fuel moisture content (FMC) for each type of dead fuel in every sample by measuring its weights using an electronic balance, and two parallel tests were performed for each sample:

$$FMC = \frac{m_1 - m_2}{m_2} \times 100\%, \quad (1)$$

where m_1 is the fresh weights (g); m_2 is the dry weights (g) [38].

2.3.2. Determination of HHV

The higher heating value (HHV) refers to the heat released by the complete combustion of a unit weight of dead fuel in an adiabatic state at room temperature. The HHV of the samples was determined using an XRY-1C softcomputer oxygen bomb calorimeter. For this, 1 g of the dried samples was weighed on a balance, and two parallel tests were realized for each sample:

$$HHV = K \frac{[(T_1 - T_2) + \Delta T]}{M}, \quad (2)$$

where K is the water equivalent, kJ/°C; T_1 is the temperature before ignition of the dead fuel, °C; T_2 is the temperature after ignition of the dead fuel, °C; ΔT is the temperature correction value, °C; and M is the weight of the sample, g [39].

2.3.3. Determination of Ash

Ash content refers to the mineral residue of the dead fuel after complete combustion. The substance retards combustion, and the higher its content, the worse the combustibility. It was analyzed using the high-temperature dry-ash method. A balance was employed to measure 1 g of the desiccated specimen. Before placement of the sample, the crucible weight was recorded. The weight of the sample and the crucible before ashing was also noted. Subsequently, the crucible containing the sample was heated in a muffle furnace with the temperature set at 800 °C for 12 h. After cooling, the samples were weighed again and the weights were documented, and two parallel tests were set up for each sample:

$$Ash = \frac{m_4 - m_5}{m_3 - m_5} \times 100\%, \quad (3)$$

where m_3 is the total weight of the sample and crucible before ashing, m_4 is the weight of the sample and crucible after ashing, and m_5 is the weight of the crucible [40].

2.3.4. Determination of Fat

Fat content is a vital metric for measuring the combustibility of dead fuel. Oil considerably promotes flame combustion, and higher oil content increases the flammability of tree species. Before the experiment, the filter paper was baked in the oven (85 °C) for 20 min to be absolutely dry, and then the weight of the filter paper was weighed with a balance and recorded. A total of 1 g of the dried sample was weighed, wrapped in the filter paper, and the weight of the filter paper and the sample was recorded. The petroleum ether was added, and then the glass container was placed in the thermostatic water bath, the time was set to 5 h, and the temperature to 85 °C. Two parallel tests were performed for each sample:

$$Fat = \frac{m_7 - m_6}{m_8 - m_6} \times 100\%, \quad (4)$$

where m_6 is the weight of the filter paper (g), m_7 is the weight of the filter paper and sample before drying, and m_8 is the weight of the filter paper and sample after drying (g) [40].

2.4. Potential Fire Behavior Testing

In this study, we simulated experiments on dead fuel behavior when burning indoors without wind. Figure 3 shows the fuel bed ($2\text{ m} \times 1.3\text{ m} \times 0.3\text{ m}$). To simulate the slope of the sample site during the field survey, 2 cm thick plasterboard was laid on the bottom of the combustion beds to reduce heat loss. Before each group of combustion experiments, the weight of dead fuels was weighed. During the eruption of the samples, the duration of visual flaming (DVF) was recorded with a stopwatch, while the vertical flame height (VFH) was measured with a steel tape measure. After burning to completion, all the burnt material in the combustion bed was weighed, and the volume of the fuel consumed (VC) was calculated.

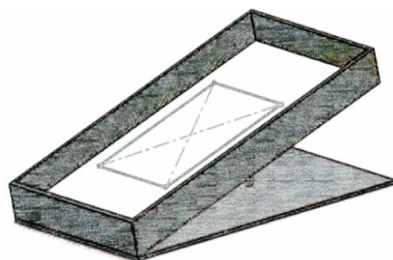


Figure 3. Diagram of the fuel bed; dead fuel was evenly distributed within the beds ($1\text{ m} \times 1\text{ m}$).

The fire-line intensity formula is defined as [41]:

$$\text{FLI} = \text{HHV} \times \text{FD} \times \text{RS}, \quad (5)$$

where FLI is fire-line intensity, kW/m , HHV is higher heating value, kJ/g , FD is the fuel load, t/ha , and RS is rate of spread, m/min .

The volume consumed formula is defined as [42]:

$$\text{VC} = \frac{\text{A} - \text{B}}{\text{A}} \times 100\%, \quad (6)$$

where A is the weight of dead fuel before burning (kg), and B is the weight of dead fuel after burning (kg).

2.5. Statistical Analysis

SPSS 22.0 (SPSS Institute, Inc., Chicago, IL, USA) statistical software was used to analyze and process the data. One-way ANOVA and least-significant difference were used to compare the significance of differences in the combustibility of dead fuels in different treatments. Pearson's correlation was used to analyze the linear correlation between combustibility. Paired samples *t*-tests were used to compare the correlation between the differences in the combustibility of dead fuels and the trends in the combustibility of dead fuels by prescribed burn removal.

3. Results

3.1. Forest Stand Characteristics of *P. yunnanensis* Forest

Table 1 provides detailed results of investigations; the mean height below the first live branch in the prescribed burn sample area exceeds 7 m, more than 1 m higher than the height in the unburned area. Varied treatment had minimal impact on *P. yunnanensis* stands. Paired sample *t*-tests revealed no significant differences ($p > 0.05$) in any of the characteristics of the *P. yunnanensis* stand.

3.2. Effect of Prescribed Burning on the *P. yunnanensis* Forest

3.2.1. Fuel Bed Structure

Figure 4 shows the vertical structure of the *P. yunnanensis* forest. The surface dead fuels in the PB plots were conifers, herbs, and dead ferns. The UB had a richer diversity of woody debris, including dead leaves, ferns, herbs, and shrubs.

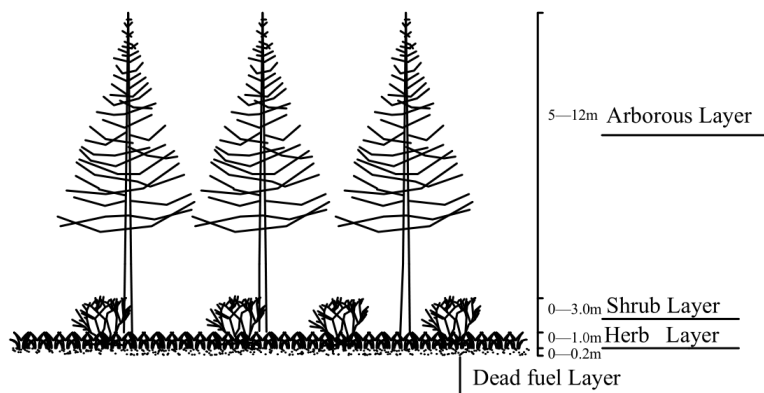


Figure 4. Fuel vertical structure of the stand from low to high dead fuel layer, herb layer, shrub layer, and arborous layer in the forest of *P. yunnanensis*.

As presented in Figure 5, the fuel moisture content (FMC) of the samples ranged from 7.02% to 20.26%, with an average of 14.41%. In comparison, the control plots had thicker surface piles with an average thickness of 4.55 cm.

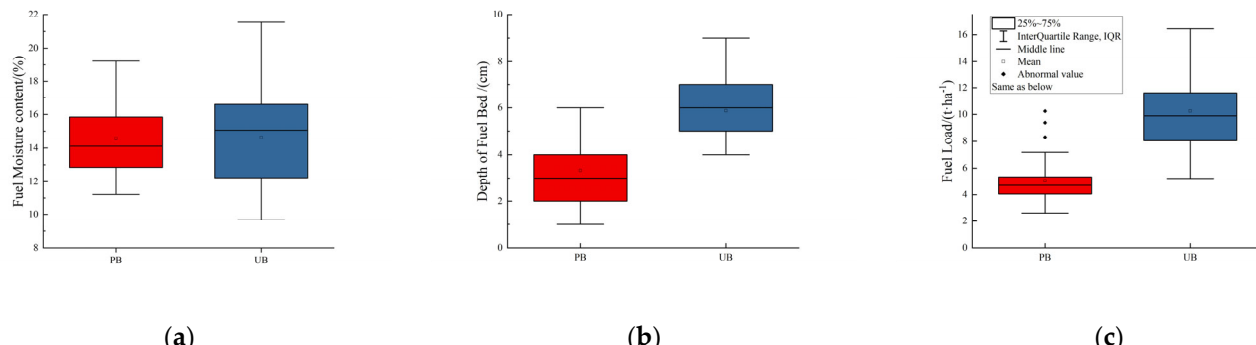


Figure 5. Comparison of (a) FMC, (b) depth of fuel bed, and (c) fuel load by burning treatment. Red represents areas affected by prescribed burning; blue represents control areas.

The shrub and herb layer height in UB was taller, and the surface fuel was thicker, which made it difficult to control the fire. The average dead fuel load of the PB decreased to 4.4 t/ha. Meanwhile, the dead fuel load of the UB was 9.8 t/ha, which was 2.22 times higher than that of the PB.

Table 2 shows that, in PB, the maximum height of herb and shrub were 59 cm and 79 cm, respectively. These measurements reveal a significant gap of over 3 m between the minimum height of the undergrowth beneath the *P. yunnanensis* branches (4.24 m) and the maximum heights of the herb and shrub. In contrast, within the UB, the maximum height of the shrub layer was recorded at 2.8 m, with less than 1 m separating it from the minimum height of the undergrowth beneath the *P. yunnanensis* branches (3.87 m), and the shrub and small tree layer act as a “ladder fuel”.

Table 2. Height and cover of herb and shrub layers by varied treatments.

Treatments	Herbaceous Cover (%)	Shrub Cover (%)	Herb Height (cm)	Shrub Height (cm)
			Mean (SE) ¹	Mean (SE) ¹
PB	75–90	25–35	48.8 (10.2) a ²	58.8 (19.9) a
UB	55–80	65–80	54.2 (7.6) a	226.2 (56.7) b

¹ Mean and one standard error (SE). ² Different lowercase letters indicate significant differences in the content of index ($p < 0.05$).

3.2.2. Physical and Chemical Properties of Surface Dead Fuel

The physical and chemical properties of surface fuel in the PB and the UB are illustrated in Figure 6. The average HHV of dead fuel in the UB is 19.56 kJ/g, and in the PB is measured at 19.64 kJ/g. The observed difference between these values is not significant. The ash content in the control sample plots was slightly higher compared with the burn-removed sample plots. The average ash content was approximately 3%, indicating better combustibility of the surface dead combustible material of *P. yunnanensis*. The ignition temperatures of surface dead fuel in the control and burned-out plots were similar at 270 °C. On average, the fat content of dead fuel on the surface of the *P. yunnanensis* forest is 9%.

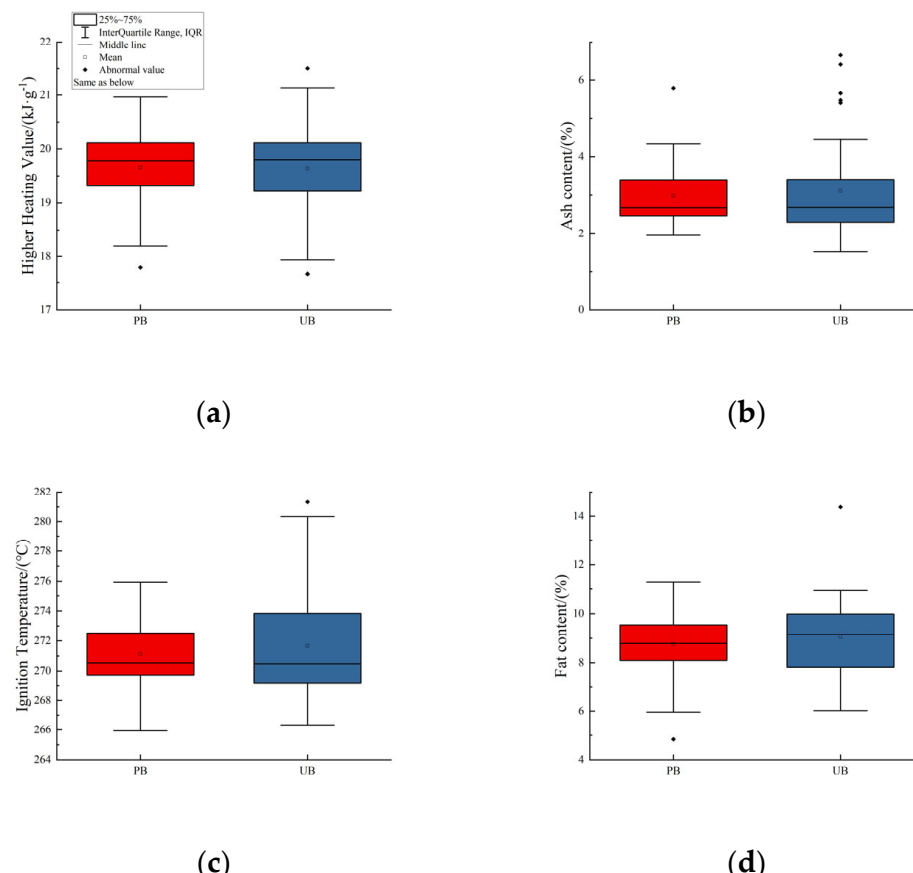


Figure 6. Comparison of physical and chemical properties: (a) higher heating value, (b) ash content, (c) ignition temperature, and (d) fat content by burning treatment. Red represents areas affected by prescribed burning; blue represents control areas.

3.2.3. Potential Fire Behavior of Surface Dead Fuels

Fire behavior variations were observed in each burn test (Figure 7).

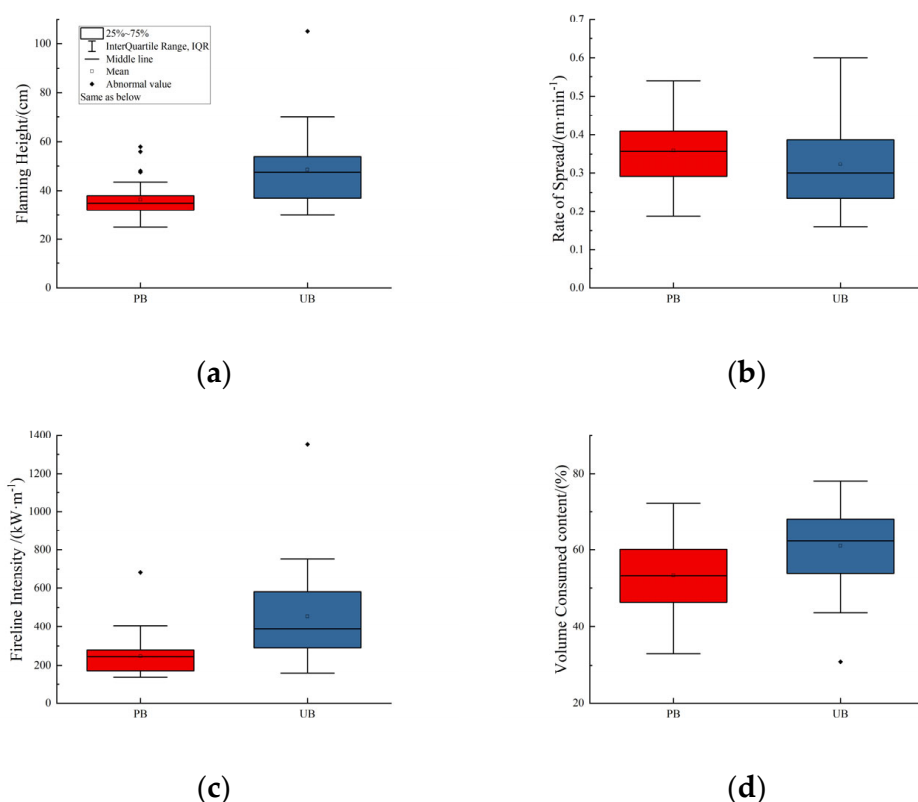


Figure 7. Comparison of fire behavior of surface fuels: (a) flaming height, (b) rate of spread, (c) fire-line intensity, and (d) volume of the fuel consumed by burning treatment. Red represents areas affected by prescribed burning; blue represents control areas.

To determine the rate of fire spread (RS), the flame maintenance duration was measured in the field. A steeper slope resulted in a greater forest fire spread rate. The RS of the PB was 0.35 m/min, while that of the UB was 0.32 m/min. However, the difference was insignificant.

The fire-line intensity is a critical aspect of forest fire behavior. When using the downhill fire ignition method, according to Byram's fire-line intensity (Equation (5)), the fire-line intensity measured less than 750 kW/m, which is classified as a low-intensity fire. The laboratory fire behavior simulation revealed the average values of fire intensity to be 247.47 kW/m (PB) and 456.12 kW/m (UB).

The volume of the fuel consumed (VC) is often used to assess the effectiveness of prescribed burning (Equation (6)). The downhill fire ignition technology, where the flame and the head of the fire move opposite to the forward direction, results in a significant combustion effect.

3.2.4. Pearson Correlation of Surface Dead Fuels

The surface dead fuel characteristics in the prescribed burning area exhibit a stronger correlation compared with the unburned area (Figure 8). FL correlated very significantly with the DFB ($p < 0.01$). HHV was highly significantly negatively correlated with ash ($p < 0.01$). In terms of fire behavior parameters, FIL exhibits the strongest correlation with VFH and RS. DFB correlates highly significantly with VFH, and FL correlates highly significantly with VFH and FLI in both PB and UB.

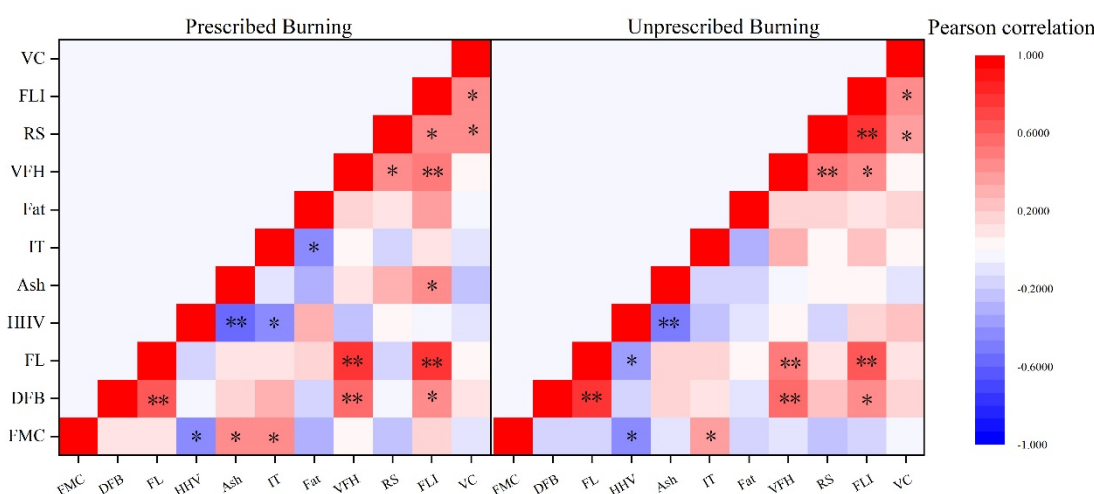


Figure 8. Pearson correlation analysis of fuel moisture content, depth of fuel bed, fuel load, higher heating value, fuel ash content, ignition temperature, fuel fat content, vertical flame height, rate of spread, fire-line intensity, and volume of the fuel consumed. Adopting abbreviations, the translation of namely FMC, DFB, FL HHV, ash, IT, fat, VFH, RS, FLI, and VC are the same as below. *: At the 0.05 level (two-tailed), the correlation was significant; **: At the 0.01 level (two-tailed), the correlation was significant.

As shown in Table 3, except for the fire spread rate, all other indicators in the UB are higher than those in the PB. Among them, DFB, FL, VFH, FLI, and VC values were significantly higher in the control site than in the burned site. When comparing the correlation between the combustibility indices, the strongest correlation was found for the fire behavior parameters, except for the fire spread rate; the other three indices reached a highly significant correlation. The following strongest correlation was for the fuel bed structure, with highly significant correlations for DFB and FL. The weakest inter-layer correlation was for physicochemical properties ($p > 0.05$), and it can be seen from Figure 6 that there was no significant change in the physicochemical properties of the dead fuels on the surface of the *P. yunnanensis* forests as a result of prescribed burning.

Table 3. Paired sample *t*-test of PB and UB.

Sample	Pairing Difference				<i>t</i>	Significance (Two Tails)	
	Average	SD	MSD	CID			
				Lower Limit	Upper Limit		
FMC	-0.0586	3.7290	0.6808	-1.4510	1.3338	-0.08	0.932
DFB	-2.533	1.8519	0.3381	-3.2248	-1.8417	-7.49	0.000
FL	-0.5188	0.3876	0.0707	-0.6635	-0.3740	-7.33	0.000
HHV	-81.4124	1328.3941	242.5304	-577.4429	414.6180	-0.33	0.740
Ash	-0.1256	1.4665	0.2677	-0.6732	0.4220	-0.46	0.642
IT	-0.5459	4.5110	0.8236	-2.2304	1.1385	-0.66	0.513
Fat	-0.2982	2.0127	0.3674	-1.0498	0.4532	-0.81	0.524
VFH	-12.0500	18.3830	3.3562	-18.9143	-5.1856	-3.59	0.001
RS	0.0361	0.1580	0.0288	-0.0228	0.0951	1.25	0.220
FLI	-208.6519	300.9631	54.9481	-321.0334	-96.2705	-3.79	0.001
VC	-11.7991	13.1720	2.4048	-16.7176	-6.8806	-4.90	0.000

SD: standard deviation; MSD: mean value of SD; CID: 95% confidence interval of difference.

3.3. Effect of Different Burn Treatments

3.3.1. Physical and Chemical Properties

Figure 9 shows the effects of different treatments of prescribed burning on the physicochemical properties of surface dead fuel on the *P. yunnanensis* forests, the indicators of

which are dead fuel ash, fat, FMC, and HHV (no comparison was made due to the lack of information on the IT of dead fuel at PB3a), with mean values of 3.81%, 6.75%, 14.69%, 19.97 kJ/g (PB3a) and 2.74%, 7.74%, 14.69%, 20.44 kJ/g (PB1a), with variations of –27.99%, 14.69%, –0.29%, and 2.35%, respectively. Different prescribed burn treatments had a significant effect on the ash and fat of dead fuel (ANOVA: ash: $F = 11.131, p < 0.001$; fat: $F = 9.091, p = 0.004$; HHV, $F = 6.835, p = 0.011$; where $p < 0.05$ difference is significant, and $p < 0.01$ indicates highly significant difference, and this is the same as below). Reducing the interval time increases the combustibility of dead fuels.

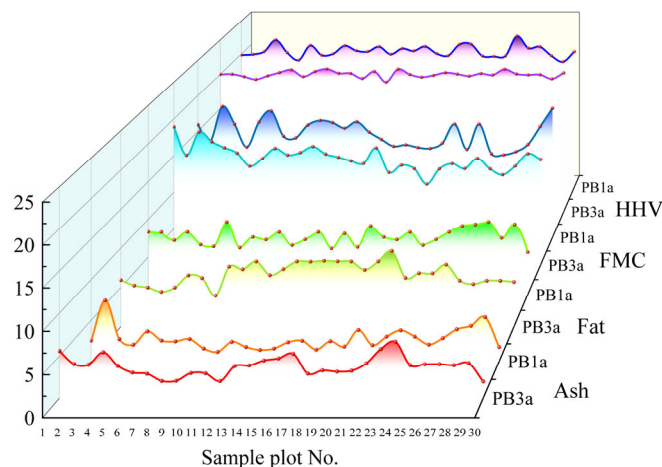


Figure 9. Physical and chemical properties (higher heating value, fuel moisture content, fat content and ash content) of dead fuel at different burn treatments. The units of ash, fat, and FMC are (%), and HHV is (kJ/g).

3.3.2. Potential Fire Behavior

To investigate the effects of different burn treatments on surface dead fuel loads and potential fire behavior, the distribution of fuel loads and their potential fire behavior was statistically compared between the 3a prescribed burn interval sample sites and the 1a prescribed burn interval sample sites, as shown in Figure 10 (ANOVA: FL: $F = 14.711, p < 0.001$; VFH: $F = 6.128, p = 0.016$; RS: $F = 1.328, p = 0.254$; FIL: $F = 3.414, p = 0.070$). Fire-line intensity varied with load (Equation (5)), decreasing from 247.47 kW/m (PB3a) to 190.56 kW/m (PB1a).

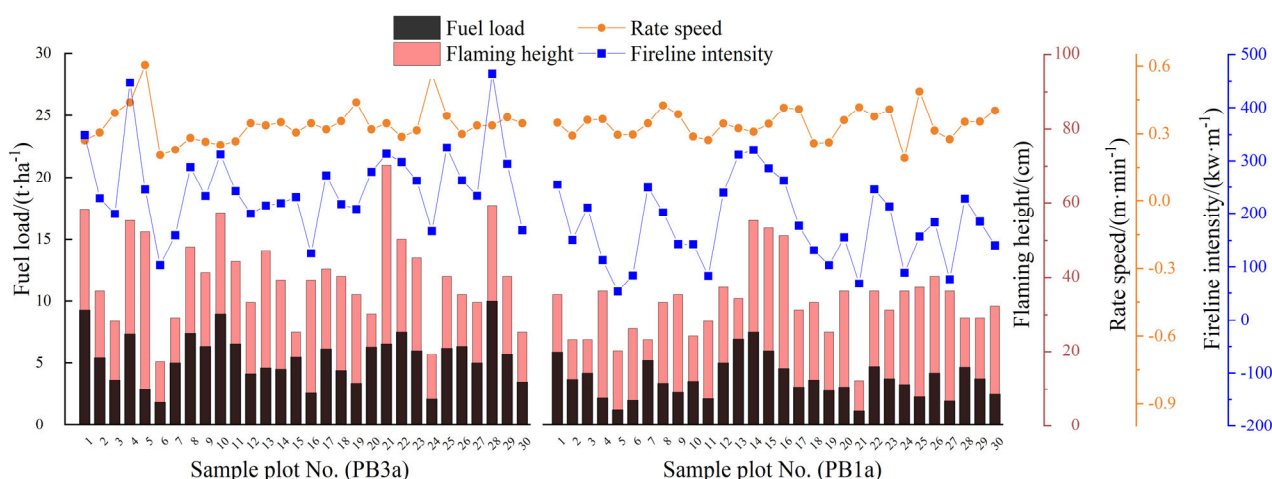


Figure 10. Fuel load and potential fire behavior of dead fuel at different burn treatments.

4. Discussion

4.1. Forest Stand Characteristics of *P. yunnanensis* Forest

The central region of Yunnan in China is recognized as a high-risk area for wildfires. In recent years, China's active forest fire prevention policy has significantly influenced the spatial and temporal characteristics as well as the intensity of wildfires. Fire-adapted traits, which characterize plant performance in the spatial fire environment, improve plant survivability under fire disturbance [43]. Through long-term adaptation, plants have evolved heritable fire-adapted traits to improve their fire adaptability during long-term adaptation to fire disturbance [44]. Short-term studies (<10 years) have shown that programmed burns have minimal effect on the mortality of canopy trees [45–47]. The mortality rate of *P. yunnanensis* under natural conditions was approximately 0.93% to 1.27%, while under prescribed burns, it was 1.33%, indicating that *P. yunnanensis* has some fire resistance and that prescribed burns on it are safe. Furthermore, regular programmed burning was shown to not affect the survival and productivity of mature coniferous forests [48–50]. Even after repeated burning over 60 years, there was minimal impact on the structure, composition, or growth of overstory trees [51]. These findings provide a scientific basis for implementing prescribed burns without altering stand age structure and the natural succession processes of forests, while concurrently reducing wildfire severity.

Frequent fire disturbance improves the fire resistance of *P. yunnanensis*, primarily through the thickening of its bark and the development of long and thick needles. The increased bark thickness provides favorable protection against the damage caused by frequent surface fires, making it less susceptible to mortality from low to medium intensity surface fires, which is an adaptive response of some species with post-fire regeneration ability [52].

In the longleaf pine ecosystems of the southeastern United States, it is generally recommended to utilize low-intensity surface fires (2–4 years). This approach helps maintain forest structure and promote understory plant diversity [53]. Repeated burns have reduced or eliminated small-diameter logs and shrubs, as observed in PB plots (Table 2). Due to the limited growth rate of vegetation and the slow accumulation of fuels, high-frequency prescribed burns may not always consume significant amounts of fuel. Instead, expanding the area burned may yield more favorable outcomes. Although scheduled burns can consume fine fuels, they do not affect coarse woody debris (CWD), which can lead to CWD build-up and high-intensity fires. Therefore, a combination of prescribed burns and mechanical treatments to remove dead fuels from the forest can minimize fire risk. Based on the fire intensity requirements of prescribed burns, and after predicting the dynamics of the net accumulation of dead fuels on the surface of the *P. yunnanensis* prescribed burn area, the appropriate frequency for implementing prescribed burning is recommended to be maintained at three to five years, and we will continue to follow up on this in future studies.

4.2. Changes in Surface Dead Fuel in *P. yunnanensis* Forests

Prescribed burning redistributed the structure of the dead fuel bed and had a significant effect on combustibility. The moisture content of the fuel plays a critical role in determining the occurrence and spread of fire. A low FMC, usually between 10–16%, is considered hazardous for flammability, and dead fuel can easily ignite [54]. Through successive years of prescribed burns, the number of surface piles resulted in an average thickness of dead fuel in the burned sample plots of 2.18 cm. As shown in Figure 4 and as Table 2 demonstrates, the burning reduced the thickness of the dead fuel bed, the herbaceous layer, and the height of the shrub layer by 42.23%, 9.96%, and 74.01%, respectively. In addition, there were also noticeable changes in the loading of surface dead fuel, with average surface dead fuel loading decreasing from 10.24 t/ha (UB) to 5.50 t/ha (3a) and 3.70 t/ha (1a), with decreases of 46.29% and 63.87%, respectively.

Physical and chemical properties of dead fuels play a crucial role in determining their burning capacity. In the laboratory, the physicochemical properties of the dead

fuel were relatively stable, with an average calorific value of medium calorific value (15–20 kJ/g), and a part of it reached a high calorific value (>20 kJ/g), which releases more energy during combustion. The ignition temperature usually decides whether the combustible material is inflammable or not. The research reveals that the maximum temperature of the top surface of a lit cigarette is 289 °C; cigarette butts can easily ignite the surface fuel of *P. yunnanensis* forests. If the fat content is more significant than 6%, it is considered a high oil content [54]. It is evident that the dead fuel on the surface of *P. yunnanensis* is highly flammable. There was no significant impact of prescribed burning removal on the physicochemical properties of dead fuel on the surface of *P. yunnanensis* ($p > 0.05$).

Understanding fire behavior indicators, such as VFH, RS, and FLI, for surface dead fuel can aid forest fire managers in deciding whether or not to proceed with prescribed burns. The UB had a greater thickness of surface dead fuel than the PB, resulting in significantly higher flame heights. During the burning experiment in the UB, the maximum flame height reached 105 cm, which is twice the maximum height observed in the PB (58 cm). The PB was situated in sloping terrain conditions (Table 1). Large sloping terrains may cause an unpredictable fire spread process, resulting in a fire-line that spreads 10% faster than at the UB, and the VC was higher in the UB (63.85%) than the PB (52.05%). This study employed a downhill ignition technique. The reason for utilizing this technique is its potential to significantly reduce the rate of forest fire spread. It is particularly effective in steadily advancing surface fires (rate of spread $< 4 \text{ km/h}$), which ensures the safety of forest fires. The fire-line intensity of the UB (456.12 kW/m) was significantly higher than that of the PB (247.47 kW/m). The most pronounced impact of shortening the burning treatments was observed on fuel load, followed by flame height. The trends in simulated flaming height in the fuel beds were generally consistent with the fuel load at the sampled sites (Figure 10), suggesting that energy release is closely related to effective fuel loads during burning. However, there was little effect on the rate of fire spread, which varied little because the experiment was conducted on a fixed sample site with no change in terrain (slope). This demonstrates that under the prescribed burnout conditions, the pure forest of *P. yunnanensis* had low combustibility and reduced the risk of severe wildfire. The combustion experiments were carried out indoors to minimize the impact of unstable field conditions on the results.

Previous research has confirmed that slope can affect the flammability of surface dead fuel by affecting factors such as load, water content, and fire behavior [55]. However, this study found that slope has no significant effect on the physicochemical properties of surface dead fuel in *P. yunnanensis* forests. In contrast, the slope factor significantly interferes with the rate of spread and burn rate among fire behavior parameters [56]. Specifically, for the same spot-burning method, areas with small slopes exhibit more effective burning compared with steeper slopes. In future studies, expanding the slope range can help to explore further the effect of terrain factors on the combustibility of surface fuel.

4.3. Impacts on Understory Species of *P. yunnanensis* Forests

P. yunnanensis forests are characterized by their dominance of this species and their community structure, consisting of a single tree species in the canopy layer. The impact of anthropogenic disturbance did not have a significant effect on the canopy layer of *P. yunnanensis* forests. However, it did have a relatively significant impact on the shrub and herb layers. Shrub cover was significantly lower in the PB than UB site because the prescribed burn suppressed shrub growth, thereby reducing vertical continuity and effectively mitigating the risk of surface fires spreading into crown fires resulting in major wildfires, such as flying fire and other high-energy fires [57,58]. Interestingly, herb cover was higher in the burned area than in the unburned area, and herb growth was greater in the burned area as well. This can be attributed to two main factors. Firstly, the prescribed burn suppressed shrub growth, which reduced shrub cover, allowing more sunlight to reach the herbs. Secondly, the burned ash in

the burned area provided additional nutrients to the herbs. Similar to many previous studies, prescribed burns increased the height of herbaceous plants in the understory vegetation [59,60]. However, it is worth noting that prescribed burning did not lead to an increase in plant species richness, as observed in the study by Arévalo et al. [61]. According to Wayman's study [62], fire disturbance was the most effective measure to reduce shrub cover. The prescribed burns resulted in a suppression of oak plants, the primary dominant species in the *P. yunnanensis* understory, and a decrease in the shrub layer's mean height and mean cover [36]. While the bark thickness of 25-year-old *P. yunnanensis* individuals can withstand surface fires, oak trees require more than 60 years to develop the necessary bark thickness. Therefore, prescribed burns can be employed to reduce the stand density within mature *P. yunnanensis* forests. If the flame heights exceed the height of the first limb below, low limbs, and shrubs, they can act as ladder fuels and potentially facilitate the spread of fire to the canopy. As shown in Table 2, the prescribed burn area has a significantly lower shrub layer height compared with the unburn area. This reduction in height decreases the vertical continuity of fuels in the forest, weakening the probability of a surface fire escalating into a canopy fire. Therefore, prescribed burns help to prevent major forest fires.

4.4. Management Implications

In 2017, our research team initiated a locational and tracking study spanning multiple years in the *P. yunnanensis* forest located in Zhaobi Mountain, Yunnan Province (Figure 11). Previous research has predominantly concentrated on post-fire recovery [35], seed dynamics of canopy [20], and the characteristics of soil respiration [63]. However, our study responses to prescribed burning in a purely *P. yunnanensis* forest and provides insights into the effects of burning on this specific forest ecosystem. To assess the combustion characteristics of surface dead fuel, a field test was conducted to remove prescribed burns. Downhill fire ignition technology was used during the process, and several technical indicators were achieved that exceeded the *P. yunnanensis* prescribed burn removal specification requirements. The results of the study guide actual forest fire management work. In contrast to developed forestry countries such as the United States and Australia, China relies more heavily on manual labor for prescribed burning, posing a significant test of personal experience. Simultaneously, the burning process poses a risk to those carrying it out. Therefore, with regards to prescribed burns in the forests of southwest China, we recommend that further research concentrate on: (1) Continuing to locate and study prescribed burns, proposing improved ignition techniques and intervals, among other factors; (2) Considering the smoke emissions during the combustion process, including the composition and content of smoke created by centralized and contiguous burns, as well as studying their migration and dissipation patterns, to diminish the air pollution caused by prescribed burns; (3) Collaborating with firefighters and employing drones to implement spot burns and carry out real-time monitoring; (4) Utilizing drones to monitor the burns in real time. Using firefighters to conduct spot burns and monitor environmental conditions in real time, including wind speed and direction; and (5) Referring to the results of China's First Natural Disaster Risk Census (2021) and the recent round of the regional forest fire risk level to determine the safe and efficient prescribed burning and removal. By addressing these research areas, we can enhance prescribed burning practices in the forests of southwest China, improving both efficiency and safety.

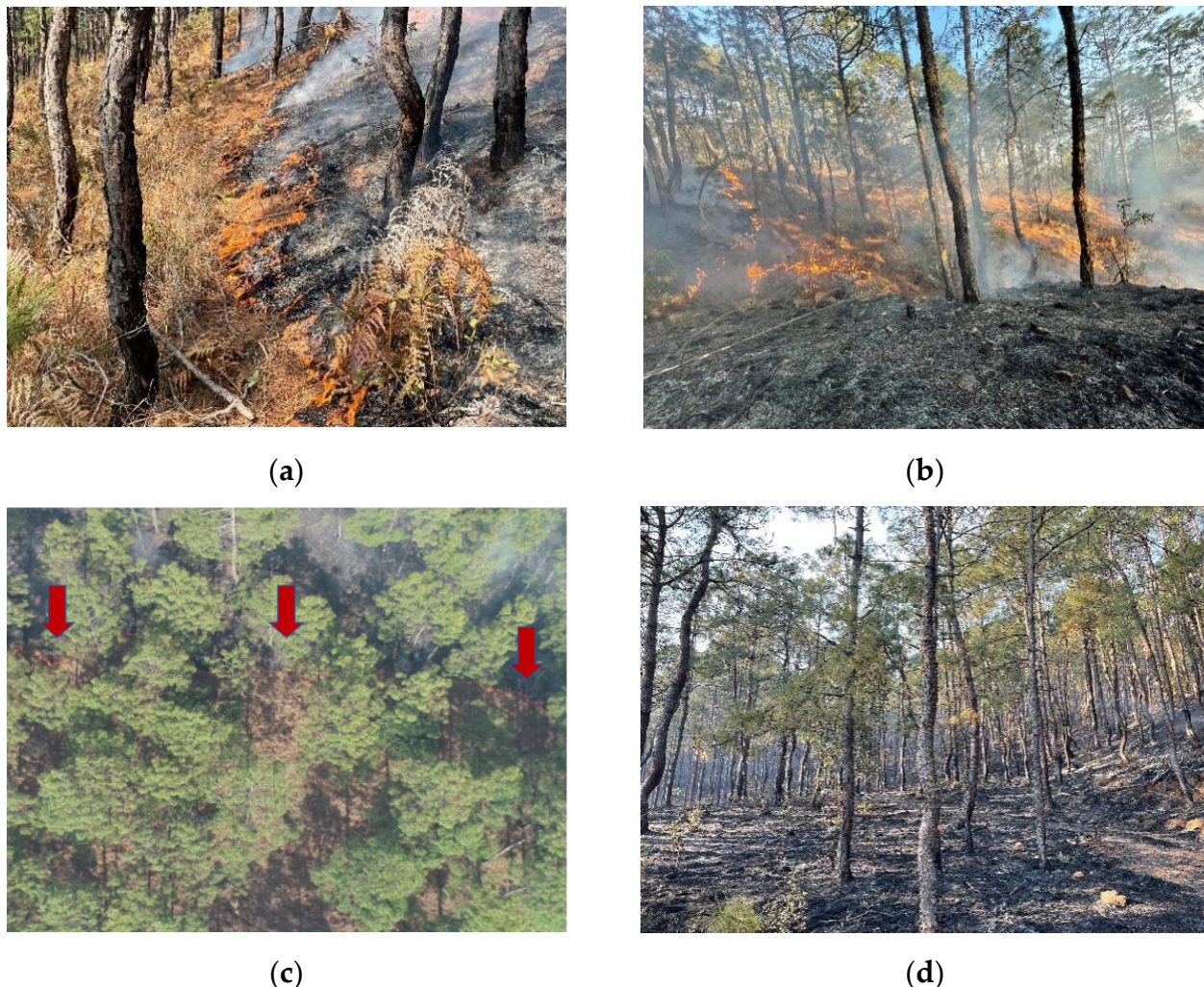


Figure 11. Images of prescribed burning in *P. yunnanensis* forest: (a–c) prescribed burning; (c) the red arrow indicates the direction of flame spread; (d) forest after the fire.

5. Conclusions

This study delved into the impact of prescribed burning on the flammability and potential fire behavior of dead fuels on the surface of *P. yunnanensis* forests from the perspective of forest combustion science. The combustibility of dead fuels on the surface of *P. yunnanensis* forest was evaluated from three indices: dead fuel bed structure, physical and chemical properties, and fire behavior parameters. The results were as follows: (1) prescribed burning has been demonstrated as an effective method for suppressing the growth of understory shrubs of *P. yunnanensis*, reducing the risk of crown fires, and is unlikely to cause large forest fires; (2) prescribed burning can effectively regulate the surface dead fuel, particularly in terms of fuel load, and the average load after burning was 4.4 t/ha, less than half of the average load in the unburned area; and (3) there were no significant differences ($p > 0.05$) among the characteristics of *P. yunnanensis* forest stands for the implementation of prescribed burning. In conclusion, the implementation of low-intensity prescribed burning is vital for regulating dead fuel under *P. yunnanensis* forests and maintaining regional carbon balance in the southwestern forest area. Moreover, it can significantly reduce *P. yunnanensis* flammability. Considering the potential for long-term fire disturbance, it is both necessary and feasible to periodically conduct prescribed burns in fire-prone habitats and fire-adapted forest stands.

Author Contributions: J.W. and Q.W. were responsible for study conception and design; R.H., C.M., X.Z., S.X., Y.T., X.L., X.Y. and Q.W. performed the experiments; J.W. and R.H. were responsible for data analysis, interpretation of results, and draft manuscript preparation; and L.W. and Q.W. revised and edited the manuscript. All authors have read and agreed to the published version of the manuscript.

Funding: This research was funded in part by the National Natural Science Foundation of China (grant number 32160376, 31960318, 31901322), the Key Development and Promotion Project of Yunnan Province (grant number 202202AD080010), the Key Laboratory of Forest Disaster Warning and Control in Yunnan Province (grant number ZKJS-S-202209), and Scientific Research Foundation of Yunnan Provincial Department of Education (grant number 2022Y606).

Data Availability Statement: Not applicable.

Acknowledgments: We thank Pu, Jun; Bai, Wanhui; Zhang, Xiyuan; and the Forestry and Grassland Bureau of Xinping County for providing field survey assistance, and the 2023 Fire Engineering undergraduate students of Southwest Forestry University for their support of this experiment.

Conflicts of Interest: The authors declare no conflict of interest.

References

- Wu, Z.; He, H.S.; Keane, R.E.; Zhu, Z.; Shan, Y. Current and future patterns of forest fire occurrence in China. *Int. J. Wildland Fire* **2020**, *29*, 104. [[CrossRef](#)]
- Urbanski, S. Wildland fire emissions, carbon, and climate: Emission factors. *For. Ecol. Manag.* **2014**, *317*, 51–60. [[CrossRef](#)]
- Arroyo, L.A.; Pascual, C.; Manzanera, J.A. Fire models and methods to map fuel types: The role of remote sensing. *For. Ecol. Manag.* **2008**, *256*, 1239–1252. [[CrossRef](#)]
- Zylstra, P. Flammability dynamics in the Australian Alps: Fact sheet. *Austral Ecol.* **2018**, *12*, 594.
- Keeley, J.E. Ecology and evolution of pine life histories. *Ann. For. Sci.* **2012**, *69*, 445–453. [[CrossRef](#)]
- Pausas, J.G. Evolutionary fire ecology: Lessons learned from pines. *Trends Plant Sci.* **2015**, *20*, 318–324. [[CrossRef](#)]
- Tian, X.; Shu, L.; Zhao, F.; Wang, M. Forest Fire Danger Changes for Southwest China under Future Scenarios. *Sci. Silvae Sin.* **2012**, *48*, 121–125+192–193.
- Wang, Q.; Shan, B.; Gong, J.; Pu, J. A Study on Prescribed Burning in Pure Forest of *Pinus yunnanensis* Franch in Central Yunnan Province. *Acta Agric. Univ. Jiangxiensis* **2018**, *40*, 235–240.
- Su, W.; Si, H.; Zhang, H.; Guo, Z. Fire-adapted traits of four pine trees in the southwestern China. *Acta Ecol. Sin.* **2023**, *43*, 1064–1072.
- Casals, P.; Valor, T.; Besalú, A.; Molina-Terrén, D. Understory fuel load and structure eight to nine years after prescribed burning in Mediterranean pine forests. *For. Ecol. Manag.* **2016**, *362*, 156–168. [[CrossRef](#)]
- Pereira, P.; Úbeda, X.; Martin, D.; Mataix-Solera, J.; Guerrero, X.C. Effects of a low severity prescribed fire on water-soluble elements in ash from a cork oak (*Quercus suber*) forest located in the northeast of the Iberian Peninsula. *Environ. Res.* **2011**, *111*, 237–247. [[CrossRef](#)] [[PubMed](#)]
- Bassett, T.J.; Landis, D.A.; Brudvig, L.A. Effects of experimental prescribed fire and tree thinning on oak savanna understory plant communities and ecosystem structure. *For. Ecol. Manag.* **2020**, *464*, 118047. [[CrossRef](#)]
- Valor, T.; Casals, P.; Altieri, S.; González-Olabarria, J.R.; Piqué, M.; Battipaglia, G. Disentangling the effects of crown scorch and competition release on the physiological and growth response of *Pinus halepensis* Mill using d13C and d18O isotopes. *For. Ecol. Manag.* **2018**, *424*, 276–287. [[CrossRef](#)]
- Molina, J.R.; Ortega, M.; Silva, F.R.Y. Scorch height and volume modeling in prescribed fires: Effects of canopy gaps in *Pinus pinaster* stands in Southern Europe. *For. Ecol. Manag.* **2021**, *506*, 119979. [[CrossRef](#)]
- Javier, M.; Gustavo, M.L.; de Nascimento, R.; Otto, A. Understanding long-term post-fire regeneration of a fire-resistant pine species. *Ann. For. Sci.* **2015**, *72*, 609–619.
- Wu, Z.; He, H.; Liu, Z.; Liang, Y. Comparing fuel reduction treatments for reducing wildfire size and intensity in a boreal forest landscape of northeastern China. *Sci. Total Environ.* **2013**, *454–455*, 30–39. [[CrossRef](#)]
- Kauppi, P.; Hanewinkel, M.; Lundmark, T.; Nabuurs, G.J.; Trasobares, A. *Climate Smart Forestry in Europe*; European Forest Institute: Joensuu, Finland, 2018.
- Defossé, G.E.; Loguerio, G.; Oddi, F.J.; Molina, J.C.; Kraus, P.D. Potential CO₂ emissions mitigation through forest prescribed burning: A case study in Patagonia, Argentina. *For. Ecol. Manag.* **2011**, *261*, 2243–2254. [[CrossRef](#)]
- Ewers, F.W. Secondary growth in needle leaves of *Pinus longaeva* (bristlecone pine) and other conifers: Quantitative data. *Am. J. Bot.* **1982**, *69*, 1552–1559. [[CrossRef](#)]
- Su, W.; Zhang, J.; Shi, G.; Wang, Z.; Zhao, L.; Zhou, R. Comparison of the canopy and soil seed banks of *Pinus yunnanensis* in central Yunnan, China. *For. Ecol. Manag.* **2019**, *437*, 41–48. [[CrossRef](#)]
- Altangerel, K.; Kull, C.A. The prescribed burning debate in Australia: Conflicts and compatibilities. *J. Environ. Plan. Manag.* **2013**, *56*, 103–120. [[CrossRef](#)]

22. Arévalo, J.R.; Bernardos, M.; González-Montelongo, C.; Grillo, F. Prescribed Burning Effect on the Richness, Diversity and Forest Structure of an Endemic Reforested *Pinus canariensis* Stand (Canary Islands). *Fire* **2023**, *6*, 150. [[CrossRef](#)]
23. Liu, X.; Huey, L.G.; Yokelson, R.J.; Selimovic, V.; Simpson, I.J.; Müller, M.; Jimenez, J.L.; Campuzano-Jost, P.; Beyersdorf, A.J.; Blake, D.R. Airborne measurements of western US wildfire emissions: Comparison with prescribed burning and air quality implications. *J. Geophys. Res. Atmos.* **2017**, *122*, 6108–6129. [[CrossRef](#)]
24. Shakesby, R.A.; Bento, C.P.M.; Ferreira, C.S.S.; Ferreira, A.J.D.; Stoof, C.R.; Urbanek, E.; Walsh, R.P.D. Impacts of prescribed fire on soil loss and soil quality: An assessment based on an experimentally-burned catchment in central Portugal. *Catena* **2015**, *128*, 278–293. [[CrossRef](#)]
25. Hu, T.; Zhao, B.; Li, F.; Dou, X.; Hu, H.; Sun, L. Effects of fire on soil respiration and its components in a Dahurian larch (*Larix gmelinii*) forest in northeast China: Implications for forest ecosystem carbon cycling. *Geoderma* **2021**, *402*, 115273. [[CrossRef](#)]
26. Hu, T.; Sun, L.; Hu, H.; Guo, F. Effects of fire disturbance on soil respiration in the non-growing season in a *Larix gmelinii* forest in the Daxing'an Mountains, China. *PLoS ONE* **2017**, *12*, e0180214. [[CrossRef](#)]
27. Alexander, H.D.; Arthur, M.A.; Loftis, D.L.; Green, S.R. Survival and growth of upland oak and co-occurring competitor seedlings following single and repeated prescribed fires. *For. Ecol. Manag.* **2008**, *256*, 1021–1030. [[CrossRef](#)]
28. Bradshaw, S.D.; Dixon, K.W.; Lambers, H.; Cross, A.T.; Hopper, S.D. Understanding the long-term impact of prescribed burning in mediterranean-climate biodiversity hotspots, with a focus on south-Western Australia. *Int. J. Wildland Fire* **2018**, *27*, 643. [[CrossRef](#)]
29. Batista, E.K.; Figueira, J.E.; Solar, R.R.; de Azevedo, C.S.; Beirão, M.V.; Berlinck, C.N.; Brandão, R.A.; de Castro, F.S.; Costa, H.C.; Costa, L.M. In Case of Fire, Escape or Die: A Trait-Based Approach for Identifying Animal Species Threatened by Fire. *Fire* **2023**, *6*, 242. [[CrossRef](#)]
30. Battaglia, M.A.; Smith, F.W.; Shepperd, W.D. Can prescribed fire be used to maintain fuel treatment effectiveness over time in Black Hills ponderosa pine forests? *For. Ecol. Manag.* **2008**, *256*, 2029–2038. [[CrossRef](#)]
31. Prichard, S.J.; Kennedy, M.C.; Wright, C.S.; Cronan, J.B.; Ottmar, R.D. Predicting forest floor and woody fuel consumption from prescribed burns in southern and western pine ecosystems of the United States. *Data Brief* **2017**, *15*, 328–338. [[CrossRef](#)]
32. Westerling, A.L.; Hidalgo, H.G.; Cayan, D.R.; Swetnam, T.W. Warming and Earlier Spring Increase Western U.S. Forest Wildfire Activity. *Science* **2006**, *313*, 940–943. [[CrossRef](#)]
33. Moreira, F.; Viedma, O.; Arianoutsou, M.; Curt, T.; Koutsias, N.; Rigolot, E.; Barbat, A.; Corona, P.; Vaz, P.; Xanthopoulos, G.; et al. Landscape—Wildfire interactions in southern Europe: Implications for landscape management. *J. Environ. Manag.* **2011**, *92*, 2389–2402. [[CrossRef](#)]
34. Tapias, R.; Climent, J.; Pardos, J.A.; Gil, L. Life histories of Mediterranean pines. *Plant Ecol.* **2004**, *171*, 53–68. [[CrossRef](#)]
35. Tang, C.Q.; He, L.Y.; Su, W.H.; Zhang, G.F.; Wang, H.C.; Peng, M.C.; Wu, Z.L.; Wang, C.Y. Regeneration, recovery and succession of a *Pinus yunnanensis* community five years after a mega-fire in central Yunnan, China. *For. Ecol. Manag.* **2013**, *294*, 188–196. [[CrossRef](#)]
36. Hong, R.; Li, J.; Wang, J.; Zhu, X.; Li, X.; Ma, C.; Cao, H.; Wang, L.; Wang, Q. Effects of prescribed burning on understory *Quercus* species of *Pinus yunnanensis* forest. *Front. For. Glob. Chang.* **2023**, *6*, 1208682. [[CrossRef](#)]
37. Reich, R.M.; Lundquist, J.E.; Bravo, V.A. Spatial models for estimating fuel loads in the Black Hills, South Dakota, USA. *Int. J. Wildland Fire* **2004**, *13*, 119–129. [[CrossRef](#)]
38. Bowyer, P.; Danson, F.M. Sensitivity of spectral reflectance to variation in live fuel moisture content at leaf and canopy level. *Remote Sens. Environ.* **2004**, *92*, 297–308. [[CrossRef](#)]
39. Wang, J.; Zhang, W.; Wang, Q.; Cao, H. Study on the burning behavior of surface fuels of sprouting *Quercus variabilis* in central Yunnan province. *Fire Sci. Technol.* **2022**, *41*, 1133–1137.
40. Wang, L.; Yang, G.; Gang, J. Changes in the Flammability of Post-Fire Aboveground Litter of *Larix gmelinii*. *Sci. Silvae Sin.* **2022**, *58*, 110–121.
41. Byram, G. Combustion of forest fuels. In *Forest Fire: Control and Use*; Davis, K.P., Ed.; Oxford University Press: Oxford, UK, 1959; pp. 61–89.
42. Wang, J.; Zhang, W.; Wang, Q. Characteristics of fire behavior in prescribed burning under *Pinus yunnanensis* forest. *J. Zhejiang A F Univ.* **2023**, *40*, 828–835. [[CrossRef](#)]
43. He, T.; Belcher, C.M.; Lamont, B.B.; Lim, S.L. A 350-million-year legacy of fire adaptation among conifers. *J. Ecol.* **2016**, *104*, 352–363. [[CrossRef](#)]
44. McLaughlan, K.K.; Higuera, P.E.; Miesel, J.; Rogers, B.M.; Schweitzer, J.; Shuman, J.K.; Tepley, A.J.; Varner, J.M.; Veblen, T.T.; Adalsteinsson, S.A. Fire as a fundamental ecological process: Research advances and frontiers. *J. Ecol.* **2020**, *108*, 2047–2069. [[CrossRef](#)]
45. Lettow, M.C.; Brudvig, L.A.; Bahlai, C.A.; Landis, D.A. Oak savanna management strategies and their differential effects on vegetative structure, understory light, and flowering forbs. *For. Ecol. Manag.* **2014**, *329*, 89–98. [[CrossRef](#)]
46. Schwilke, D.W.; Keeley, J.E.; Knapp, E.E.; Mciver, J.; Bailey, J.D.; Fettig, C.J.; Fiedler, C.E.; Harrod, R.J.; Moghaddas, J.J.; Outcalt, K.W. The national Fire and Fire Surrogate study: Effects of fuel reduction methods on forest vegetation structure and fuels. *Ecol. Appl. A Publ. Ecol. Soc. Am.* **2009**, *19*, 285–304. [[CrossRef](#)]
47. Stan, A.B.; Rigg, L.S.; Jones, L.S. Dynamics of a Managed Oak Woodland in Northeastern Illinois. *Nat. Area News* **2006**, *26*, 187–197. [[CrossRef](#)]

48. Willis, J.L.; Sharma, A.; Kush, J.S. Seasonality of Biennial Burning Has No Adverse Effects on Mature Longleaf Pine Survival or Productivity. *Front. For. Glob. Chang.* **2021**, *4*, 684087. [[CrossRef](#)]
49. Mantgem, P.J.V.; Stephenson, N.L.; Knapp, E.; Battles, J.; Keeley, J.E. Long-term effects of prescribed fire on mixed conifer forest structure in the Sierra Nevada, California. *For. Ecol. Manag.* **2011**, *261*, 989–994. [[CrossRef](#)]
50. Arkle, R.S.; Pilliod, D.S.; Welty, J.L. Pattern and process of prescribed fires influence effectiveness at reducing wildfire severity in dry coniferous forests. *For. Ecol. Manag.* **2012**, *276*, 174–184. [[CrossRef](#)]
51. Knapp, B.O.; Stephan, K.; Hubbart, J.A. Structure and composition of an oak-hickory forest after over 60 years of repeated prescribed burning in Missouri, USA. *For. Ecol. Manag.* **2015**, *344*, 95–109. [[CrossRef](#)]
52. Pausas, J.G.; Moreira, B. Flammability as a biological concept. *New Phytol.* **2012**, *194*, 610–613. [[CrossRef](#)]
53. Lear, D.H.V.; Carroll, W.D.; Kapeluck, P.R.; Johnson, R. History and restoration of the longleaf pine-grassland ecosystem: Implications for species at risk. *For. Ecol. Manag.* **2005**, *211*, 150–165. [[CrossRef](#)]
54. Wang, Q. Study on Fire Behaviors in Forest Burning. Ph.D. Thesis, Chinese Academy of Forestry, Beijing, China, 2011.
55. Certini, G. Effects of fire on properties of forest soils: A review. *Oecologia* **2005**, *143*, 1–10. [[CrossRef](#)]
56. Gautam, S.; Pulkki, R.; Shahi, C.; Leitch, M. Fuel quality changes in full tree logging residue during storage in roadside slash piles in Northwestern Ontario. *Biomass Bioenergy* **2012**, *42*, 43–50. [[CrossRef](#)]
57. Manzello, S.L.; Maranghides, A.; Mell, W.E. Firebrand generation from burning vegetation. *Int. J. Wildland Fire* **2007**, *16*, 458–462. [[CrossRef](#)]
58. Manzello, S.L.; Cleary, T.G.; Shields, J.R.; Maranghides, A.; Mell, W.; Yang, J.C. Experimental investigation of firebrands: Generation and ignition of fuel beds. *Fire Saf. J.* **2008**, *43*, 226–233. [[CrossRef](#)]
59. Hutchinson, T.F.; Sutherland, E.K.; Yaussy, D.A. Effects of repeated prescribed fires on the structure, composition, and regeneration of mixed-oak forests in Ohio. *For. Ecol. Manag.* **2005**, *218*, 210–228. [[CrossRef](#)]
60. Peterson, D.W.; Reich, P.B. Fire frequency and tree canopy structure influence plant species diversity in a forest-grassland ecotone. *Plant Ecol.* **2008**, *194*, 5–16. [[CrossRef](#)]
61. Arévalo, J.R.; Fernández Lugo, S.; Naranjocigala, A.; Salas, M.; Ruíz, R.; Ramos, R.; Moreno, M. Post-fire recovery of an endemic Canarian pine forest. *Int. J. Wildland Fire* **2014**, *23*, 403–409. [[CrossRef](#)]
62. Wayman, R.B.; North, M. Initial response of a mixed-conifer understory plant community to burning and thinning restoration treatments. *For. Ecol. Manag.* **2007**, *239*, 32–44. [[CrossRef](#)]
63. Jixia, Z.; Shaojun, W.; Qibo, C.; Yanxia, W.; Haoqin, X. Soil respiration and its affecting factors in young and mature forests of *Pinus yunnanensis* in middle Yunnan plateau, China. *J. Nanjing For. Univ. (Nat. Sci. Ed.)* **2014**, *57*, 71–76.

Disclaimer/Publisher’s Note: The statements, opinions and data contained in all publications are solely those of the individual author(s) and contributor(s) and not of MDPI and/or the editor(s). MDPI and/or the editor(s) disclaim responsibility for any injury to people or property resulting from any ideas, methods, instructions or products referred to in the content.